On the force-controlled assembly operations of a new parallel kinematics manipulator

Massimo Callegari and Alessandra Suardi

***Abstract*—Assembly tasks have been studied by many researchers for a long time, but the accomplishment of effective assembly operations still deserves more research efforts in many cases: a new parallel kinematics machine has been proposed for this kind of tasks and an hybrid position/force controller has been synthesised for the execution of operations constrained by the contact with the environment. In this paper the architecture of the system is briefly explained, then its dynamic behaviour is tested in a virtual prototyping environment with reference to the well-known problem of mating a cylindrical peg with a hole: a model of the operation has been developed, based on the classic studies on the subject, then an assembly planner has been implemented. The simulation results that have been obtained seem to support the opinion of the Authors about the good performances of the mechatronic system for the execution of assembly operations, especially if high velocities are not requested.**

***Index terms*—robot, hybrid position/force controller, peg-in-hole assembly, parallel kinematics machines.**

I. Introduction

Parallel kinematics machines (PKMs) are being more and more used in industrial applications, especially when the accomplishment of the tasks is based on physical interactions with the environment: in assembly operations, for instance, in-parallel actuated mechanisms are able to provide great stiffness and high accelerations, which is usually considered quite an advantage with respect to the performances of open-loop architectures.
As a matter of fact, the challenge in the design of robots interacting with the environment is characterised by the use of dynamics shaping and/or force modulation to subdue unwanted effects on manipulator's behaviour by adapting the control to the on-going duties. *Dynamics shaping* corresponds, in fact [1], to compensate systematic off-sets or drifts (which may arise due to actuation nonlinearities, mobilities inertial couplings, transmission compliance, actuation backlash, sensors' bias, or the likes), using error signals measured or computed by respect to a model of robot's dynamics. Conversely, aiming at the *force modulation*, the common hybrid approach considers strategies based on two commands (either position or force), conveniently switched to drive the arm as the duty is modified to constrained motion manoeuvres; a simpler realisation lies in the impedance control, which enables a force feedback mapped from position data, on condition that the coupling stiffness between robot and environment can be conveniently estimated.
A new kind of PKM has been conceived at the Polytechnical University of Marche, whose kinematics and design have been described elsewhere [2]; the present paper proposes a hybrid control algorithm for the execution of assembly operations and shows a few simulation results with reference to the well-known peg-in-hole task. The assembly operation has been carefully studied and modelled with reference to classic approaches [3], then an assembly planner has been purposely developed to assist the robot programmer in the set up of feasible tasks, as described in the following paragraphs.

Both Authors are within the Department of Mechanics, Università Politecnica delle Marche, Ancona, Italy.

II. Description of the Machine

Figure 1 schematically represents the functional design of a whole family of mechanisms [4], conventionally called *3-RCC* to indicate the sequence of the joints in the three (identical) limbs, starting from the fixed frame and moving towards the mobile platform. Each leg is composed by two parts coupled by a cylindrical pair (C): the lower link of each limb is connected to the frame by a revolute joint (R) while the upper one is connected to the platform by a cylindrical pair (C).

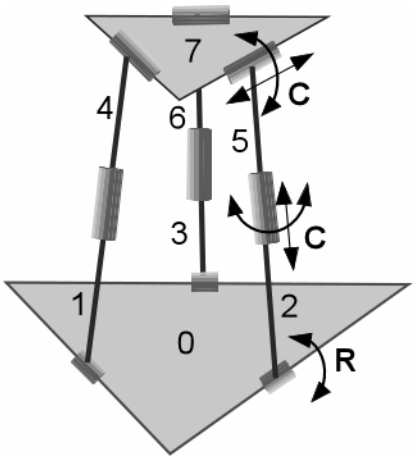

Fig. 1. Sketch of the *3-RCC* conceptual design

The described architecture is characterised by *3* d.o.f.'s and if particular geometrical configurations are satisfied such mechanisms can provide motions of pure translation: a specific machine of this kind has been further developed and its kinematics has been fully worked out in closed form, arriving at a functional

design optimised for the execution of assembly operations. As a matter of fact, quite good kinematic properties have been devised in this phase, like the relatively simple relations (characterised by only one solution in both direct and inverse problems), the convex dome-shaped workspace, free of singular points and the high stiffness at the end-effector.
A detailed design of the robot has been carried on, leading to the virtual prototype shown in Fig. 2: the dynamic simulations that have been performed showed that the high varying inertias of the machine may yield poor dynamic behaviour in the outer regions of the workspace. Therefore, while new machines are now being investigated based on the same *3-RCC* concept, a model based control has been developed to cope with the complex dynamics, as explained in the present paper; to this aim an inverse dynamic model of the robot has been derived by means of the Principle of the Virtual Works and presented already in [5].

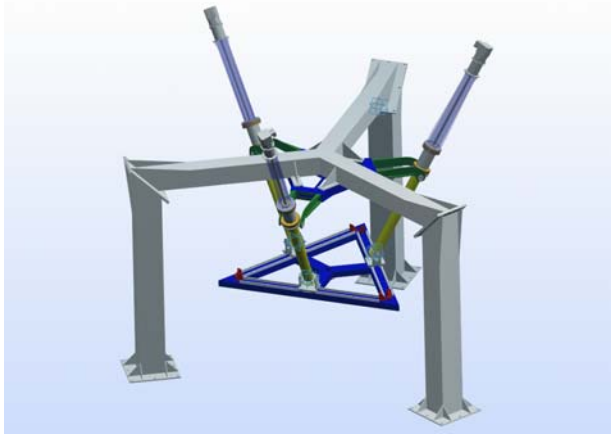

Fig. 2. CAD model of the *3-RCC* robot

III. Modelling of Assembly Tasks

In order to set up an effective simulation tool, a model of the environment was needed first; moreover, it is well known that assembly operations must be carefully planned beforehand, so a detailed study of the assembly tasks has been carried out, based on key studies on the subject [3], [6], then a computer aided planning tool has been developed. In the following sections, the well-known "peg-in-hole" task is considered, with reference to rigid parts and cylindrical pegs: both linear and smoothed chamfers have been considered, dealing with the cases shown in Fig. 3.

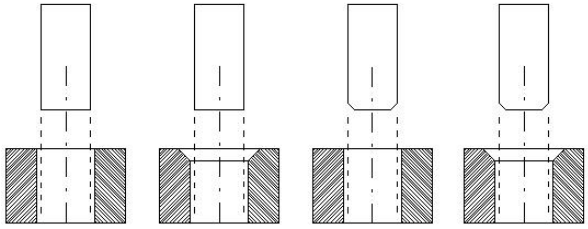

Fig. 3. Linear and smoothed chamfers for pegs and/or holes

In particular, the so-called "fine motion" assembly requires the capability of controlling both positions and contact forces with high accuracy; it develops through the following five phases, shown in Fig. 4: approach, chamfer crossing, one-point contact, two-points contact, linear contact. The outcoming models have been developed by taking into account all the relevant geometric and dynamic parameters: e.g. the chamfer crossing model, which is the simplest one, is briefly described in the following paragraphs for the quasi-static case.

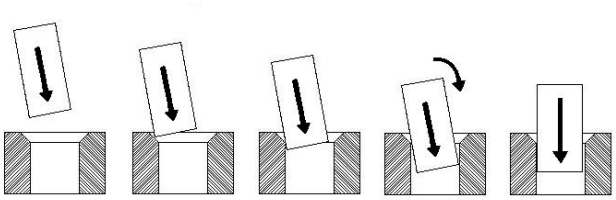

Fig. 4. The five different phases of fine-motion assembly

Looking at Fig. 5, in case of a linear chamfer the equilibrium equations provide:

$$-A\,f_1 - F_z\sin(\theta) + F_x\cos(\theta) = 0 \quad (1)$$

$$B\,f_1 - F_z\cos(\theta) - F_y\sin(\theta) = 0 \quad (2)$$

$$M - r\,f_1\left(\cos(\gamma+\theta) + \mu\sin(\gamma+\theta)\right) = 0 \quad (3)$$

having defined:

$$A = \sin(\gamma) - \mu\cos(\gamma) \qquad B = \cos(\gamma) + \mu\sin(\gamma)$$

Therefore the axial force that is needed to keep the contact between peg and hole is:

$$F_{ins} = F_z\cos(\theta) + F_x\sin(\theta) = \frac{M}{r}\,\frac{B}{B\cos(\theta) - A\sin(\theta)} \quad (4)$$

Equation (4) still holds for smoothed chamfers, provided that the actual (time-varying) contact angle γ at the contact point is considered.
Two typical problems can arise during the assembly task, both preventing the fulfilment of the operation because the peg appears stuck in the hole: the *jamming* consists in a wrong proportion among the exerted forces and moments and can occur both during one-point and two-point contact phases; the *wedging*, on the other hand, can arise only during the two-point contact phase and, deriving from a wrong geometric setting, cannot be avoided by varying the applied forces or moments. The mathematical model of both situations has been derived and useful diagrams have been drawn.

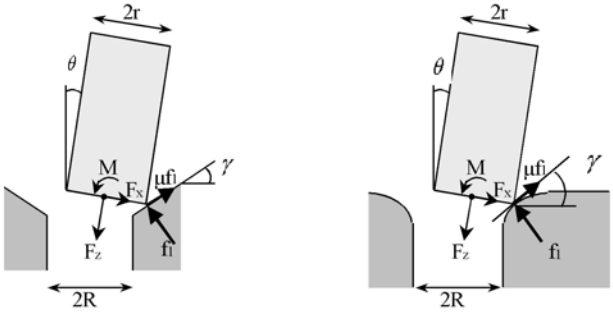

Fig. 5. Forces developed during chamfer crossing

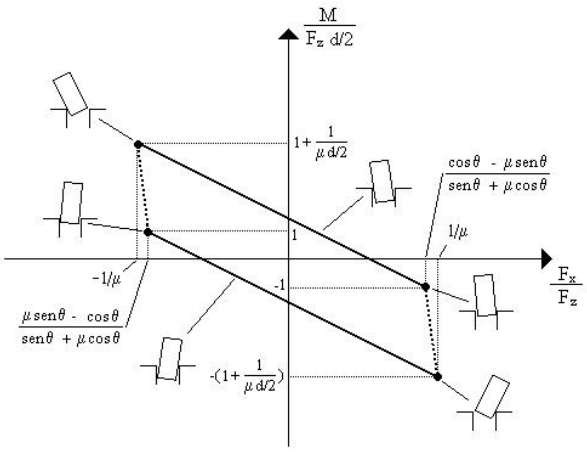

Fig. 6. Jamming diagram (absence of chamfer)

The *jamming diagram*, shown in Fig. 6, plots with solid lines the combinations of external actions, F_x, F_z ed M, that correspond to situations of equilibrium: the inside area represents a slipping region where the dynamic unbalance among the external and the reaction forces leads to successful mating of the parts, while the region outside such equilibrium lines eventually jam the peg, either in one- or two-point contact.

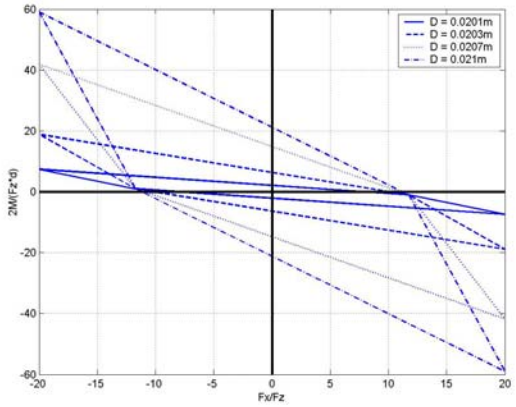

Fig. 7a. Jamming diagram for different values of hole's diameter D (μ=0.05, d=20.0 mm, θ=2°)

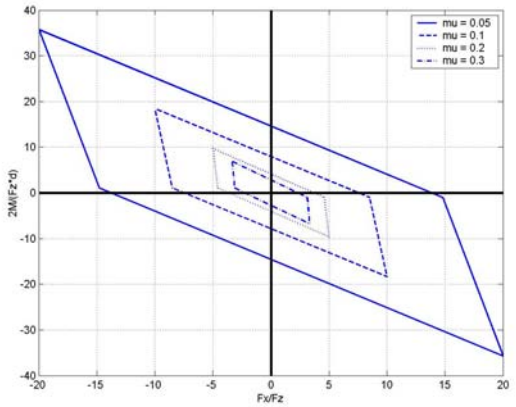

Fig. 7b. Jamming diagram for different values of static friction μ (D=20.3 mm, d=20.0 mm, θ=1°)

Once the problem at hand has been clearly identified, a sensitivity analysis can be performed to assess the impact of changes in the parameters that can still be varied during the assembly process; for instance, Fig. 7a shows the effect of variations of hole's diameter while the friction coefficient is varied in Fig. 7b. Figure 8 shows a possible situation of wedging, that occurs whether the two reaction forces act on the same line of action: if one of the two contact points lies outside the friction cone of the other, wedging does not occur. Such relation can be expressed by [7]:

$$\frac{D}{d} - \cos(\theta) - \sqrt{\left(\frac{D}{d}\right)^2 (\mu^2 + 1) - 1} \cdot \sin(\theta) > 0 \qquad (5)$$

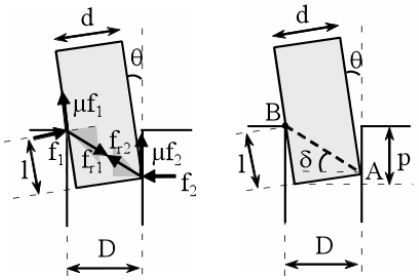

Fig. 8. Setting of reaction forces in case of wedging

If Eq. (5) is manipulated a little more, the limit values for the tilt angle θ_w or the insertion depth p_w can be found, e.g.:

$$p_w = \frac{D - d\cos(\theta_w)}{\sin(\theta_w)}\cos(\theta_w) \qquad (6)$$

Also in this case, the dependence of the critical values of the tilt angle and of the insertion depth has been assessed against variations of friction factor μ, hole's diameter D or clearance j, see Fig. 9.

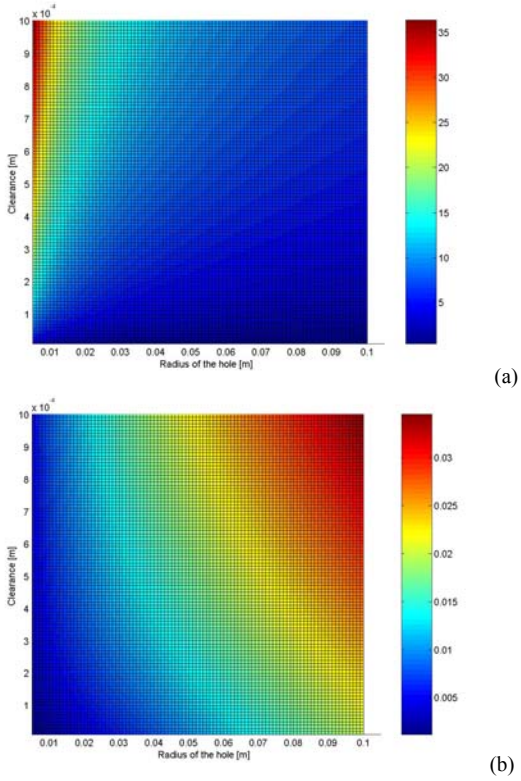

Fig. 9. Limit values for tilt angle (a) and insertion depth (b) to avoid wedging

IV. CONTROL SYSTEM

Only few studies are available on the subject of force control of parallel robots [8], [9], probably due to the fact that PKM's are relatively new architectures, characterised by quite complex kinematic and dynamic models. In this case, the theory developed for serial robots has been adapted to parallel kinematics machines, leading to the development of an implicit hybrid position/force control, as shown in Fig. 10. It is recalled that implicit methods identify the compliance of the contact through the force sensors and then compute the position and velocity control signals that correspond to the desired control force: even if some difficulties may arise in the identification of contact forces, this class of control schemes are characterised by a good robustness and easiness of implementation and therefore have been selected for the *3-RCC* robot. It must be also pointed out that in situations characterised by great uncertainties the redundancy of information provided by position and force sensors is not used properly by explicit hybrid controllers, that cancel some "channels" by means of the selection matrix. Since this thing does not happen in implicit schemes, that operate in-parallel the two position and force controllers, they are more useful for changing operating conditions.

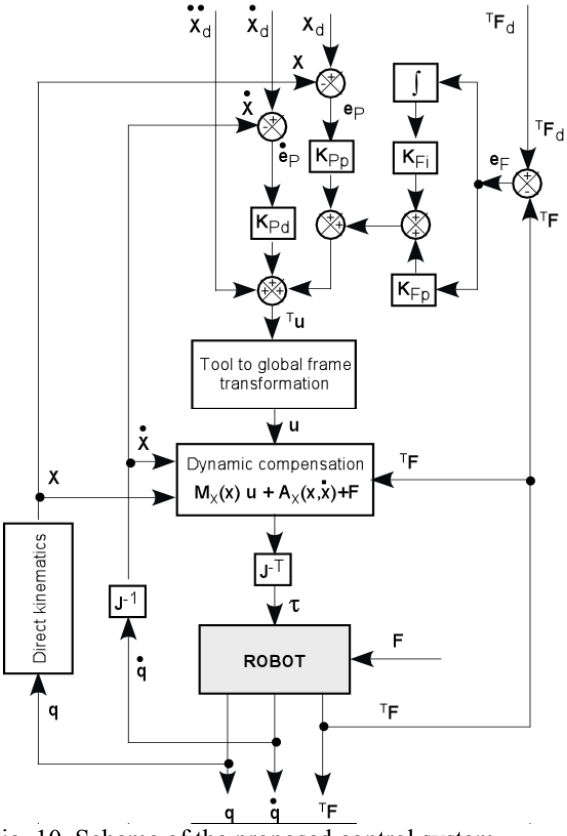

Fig. 10. Scheme of the proposed control system

Figure 10 shows the scheme of the control system that has been implemented for the simulation of the *3-RCC* robot. Force control is granted by a PI loop while position control is realised through a PD module: it is noted that, as already commented before, position reference signal is modified by the force control variable. In the inner model-based module, robot's dynamics is compensated and the external forces are taken into account as well; in fact, if an external force **F** is acting at the end-effector, robot's dynamics can be written in task-space as:

$$\boldsymbol{\tau}_{\mathbf{x}} = \mathrm{J}^{\mathrm{T}} \cdot \boldsymbol{\tau} = \mathrm{M}_{x}(\mathbf{X}) \cdot \ddot{\mathbf{X}} + \mathbf{A}_{\mathbf{x}}(\mathbf{X}, \dot{\mathbf{X}}) + \mathbf{F} \tag{7}$$

where $\boldsymbol{\tau}_x$ is the end-effector force equivalent to actual torques $\boldsymbol{\tau}$ developed at the actuated joints, M_x and $\boldsymbol{A}_x$ are respectively the manipulator's mass matrix and the vector of all other dynamic terms (gravitational, centrifugal and Coriolis forces), all expressed in task space as functions of the cartesian coordinates $\boldsymbol{X}$; it must be noted that eq. (7) is "naturally" expressed in task space X, so that the evaluation of inverse dynamics model (7), needed by the hybrid controller, is rather efficient. For the same reason, the Jacobian matrix J of parallel manipulators is usually defined the other way round with respect to serial robots:

$$\dot{\mathbf{q}} = \mathrm{J} \cdot \dot{\mathbf{X}} \tag{8}$$

Therefore, the closed-loop behaviour of the system shown in Fig. 10 can be found by composing robot's dynamics (7) with the computed actuation torques:

$$\boldsymbol{\tau} = \mathrm{J}^{-\mathrm{T}} \left(\mathrm{M}_{x}(\mathbf{X}) \cdot \mathbf{u} + \mathbf{A}_{\mathbf{x}}(\mathbf{X}, \dot{\mathbf{X}}) + \mathbf{F} \right) \tag{9}$$

and the implicit servo law:

$$\mathbf{u} = \ddot{\mathbf{X}}_{\mathbf{d}} + \mathrm{K}_{\mathrm{Pd}} \dot{\mathbf{e}}_{\mathbf{P}} + \mathrm{K}_{\mathrm{Pp}} \cdot \mathbf{e}_{\mathbf{p}} + \mathrm{K}_{\mathrm{Fp}} \mathbf{e}_{\mathbf{F}} + \mathrm{K}_{\mathrm{Fi}} \int \mathbf{e}_{\mathbf{F}} \tag{10}$$

where $\mathbf{e_p = X_d - X}$ is the position error, $\mathbf{e_F = F_d - F}$ is the force error, K_{Pd} and K_{Pp} are gain matrices for position control, K_{Fp} and K_{Fi} are gain matrices for force control. The resulting errors dynamics is governed by:

$$\ddot{\mathbf{e}}_{\mathbf{P}} + \mathrm{K}_{\mathrm{Pd}} \cdot \dot{\mathbf{e}}_{\mathbf{P}} + \mathrm{K}_{\mathrm{Pp}} \cdot \mathbf{e}_{\mathbf{P}} + \mathrm{K}_{\mathrm{Fp}} \cdot \mathbf{e}_{\mathbf{F}} + \mathrm{K}_{\mathrm{Fi}} \int \mathbf{e}_{\mathbf{F}} = 0 \tag{11}$$

Robot's tasks are usually defined in a frame $T(t_1,t_2,n)$, located at the end-effector, with n axis perpendicular to the contact surface: in this frame it is usually required the tracking of a certain trajectory along the two directions t_1 and t_2 while a force is assigned in the direction of the normal axis n. In such a task frame, Eq. (11) can be de-composed in the following manner:

$$\ddot{\mathrm{e}}_{\mathrm{P},t1} + \mathrm{k}_{\mathrm{Pd}} \cdot \dot{\mathrm{e}}_{\mathrm{P},t1} + \mathrm{k}_{\mathrm{Pp}} \cdot \mathrm{e}_{\mathrm{P},t1} = 0 \tag{12}$$

$$\ddot{\mathrm{e}}_{\mathrm{P},t2} + \mathrm{k}_{\mathrm{Pd}} \cdot \dot{\mathrm{e}}_{\mathrm{P},t2} + \mathrm{k}_{\mathrm{Pp}} \cdot \mathrm{e}_{\mathrm{P},t2} = 0 \tag{13}$$

$$\ddot{\mathrm{e}}_{\mathrm{P},n} + \mathrm{k}_{\mathrm{Pd}} \cdot \dot{\mathrm{e}}_{\mathrm{P},n} + \mathrm{k}_{\mathrm{Pp}} \cdot \mathrm{e}_{\mathrm{P},n} + \mathrm{k}_{\mathrm{Fp}} \cdot \mathrm{e}_{\mathrm{F},n} + \mathrm{k}_{\mathrm{Fi}} \int \mathrm{e}_{\mathrm{F},n} = 0 \tag{14}$$

having defined:

$$\mathrm{K}_{\mathrm{Pd}} = \mathrm{diag}\{\mathrm{k}_{\mathrm{Pd}} \;\; \mathrm{k}_{\mathrm{Pd}} \;\; \mathrm{k}_{\mathrm{Pd}}\} \quad \mathrm{K}_{\mathrm{Pp}} = \mathrm{diag}\{\mathrm{k}_{\mathrm{Pp}} \;\; \mathrm{k}_{\mathrm{Pp}} \;\; \mathrm{k}_{\mathrm{Pp}}\}$$

$$\mathrm{K}_{\mathrm{Fp}} = \mathrm{diag}\{\mathrm{k}_{\mathrm{Fp}} \;\; \mathrm{k}_{\mathrm{Fp}} \;\; \mathrm{k}_{\mathrm{Fp}}\} \quad \mathrm{K}_{\mathrm{Fi}} = \mathrm{diag}\{\mathrm{k}_{\mathrm{Fi}} \;\; \mathrm{k}_{\mathrm{Fi}} \;\; \mathrm{k}_{\mathrm{Fi}}\}$$

Equations (12) and (13) describe the dynamic behaviour of position error in the tangential directions t_1 and t_2, where the motion is unconstrained: stability is granted for any choice of the gains k_{Pd} and k_{Pp}. Equation (14), on the other hand, describes the time evolution of both position and force error in the constrained direction n. It has been shown [10] that, along such direction, the system is stable if the gains k_{Pd}, k_{Pp}, k_{Fp} and k_{Fi} satisfy the following condition:

$$\mathrm{k}_{\mathrm{Fi}} < \mathrm{k}_{\mathrm{Pd}} \left(\frac{\mathrm{k}_{\mathrm{Pp}}}{\mathrm{K}} + \mathrm{k}_{\mathrm{Fp}} \right) \tag{15}$$

where K is an estimate of contact surface stiffness. The following values have been chosen for such parameters in the present simulations (MKS units): $k_{Pd}=700$, $k_{Pp}=10\ 000$, $k_{Fp}=0.1$, $k_{Fi}=90$ and $K=10^7$.
It is remarked that, when the robot operates in unconstrained mode, the control system degrades to the positional computed torque algorithm; furthermore, the proposed control scheme, when both position and force are deviating from the required behaviour, gives a priority to the force signal, so the control actions tend to reduce the force error: such a feature can be useful in case of the occurrence of unexpected contacts which had not been considered at the time of "motion planning". In the simulations of constrained motion operations commented in the following section, the contact with the environment in the normal direction has been modelled through a non-linear hardening spring, without dampers or any other form of dissipation; in the tangential directions a dry friction has been assumed.

V. Simulation Results

To this aim, a virtual prototyping environment has been developed to study by computer simulation the performances of the robot under design, Fig. 11: the direct dynamics model of the *3-RCC* mechanism has been modelled by means of the multibody code ADAMS, Fig. 12, while the model-based controller, evaluating inverse dynamics, has been written by MATLAB/Simulink, duly interfaced to previous package by means of the ADAMS/Controls module.

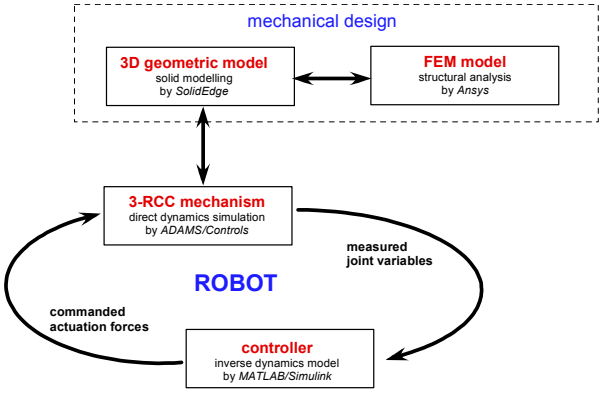

Fig. 11. Modular structure of the virtual prototyping environment

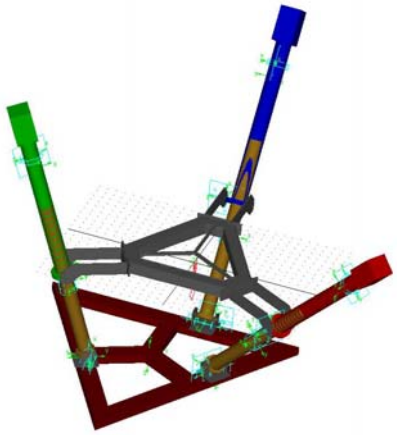

Fig. 12. Multibody model of the *3-RCC* robot

The classic benchmark for the test of assembly devices is the peg-in-hole problem: it is here made reference to the "simple" case of a cylindrical peg to be inserted into a hole with a proper chamfer (in absence of chamfer the capability to control peg's orientation would be required). Initial investigations have been performed with the peg axis parallel to hole's axis but then also the case of slight misalignments between the two parts have been studied: in this case the presence of a passive compliance at the end-effector was needed and a torsional spring with *50 Nm/rad* stiffness has been used to model the fixture. The peg has a fixed diameter of *20 mm* and a height of *80 mm*, while the mating with hole is characterised by a play of *0.08 mm* or *0.4 mm*; the chamfer has a slope of *45°* with *1.5 mm* and *3 mm* width and the error of alignment varies from *0°* to *1°*; during parts' mating, a reference force of *10 N* must be developed in the normal direction.
Figure 13a shows the contact forces in the task frame for a peg-in-hole manoeuvre with perfect alignment between peg and hole axes: peaks are evident in correspondence of hole's edges. The same behaviour can be observed in Fig. 13b, that shows the actuation torques during the same operation; Fig. 14 tracks the path travelled by the peg.

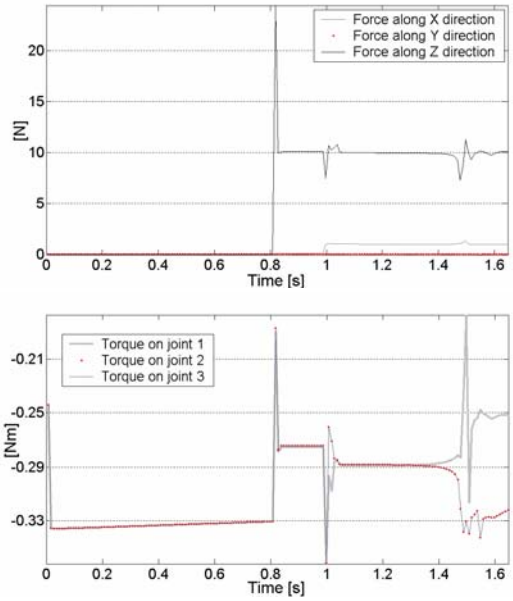

Fig. 13. Contact forces (a) and actuation torques (b) for perfect alignment

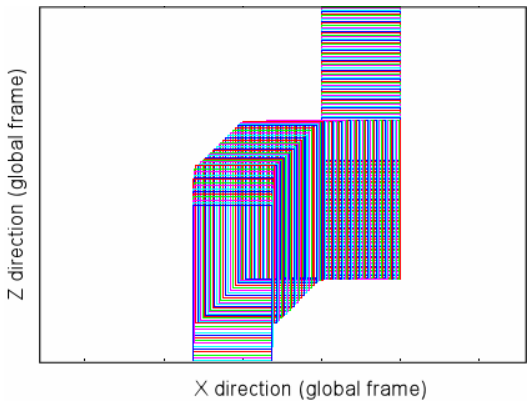

Fig. 14. Cylinder's path (no misalignment)

The following figures show what happens when a misalignment error of *1°* is introduced: the trend of contact forces and actuation torques, Fig. 15, is similar to previous case; peg's tilt angle, on the other hand, Fig. 16, increases much during the approach towards the centre of the hole (but always stays below the wedging threshold); once again chamfer's crossing results a critical phase of the assembly manoeuvre. The developed contact forces always satisfy the jamming condition in both cases.
In conclusion, the performed tests showed that the proposed control algorithm is able to perform the peg-in-hole assembly, always granting the contact between the two mating parts, even if during chamfer crossing the desired force is hardly maintained. It has also been shown that, if the end-effector orientation is not controlled, misalignments greater than *3°* lead to the practical impossibility to complete the manoeuvre. Finally, it is highlighted that the total cycle times to complete the assembly are rather high, i.e. the velocities must be pretty slow, especially if compared with passive compliance devices; such performance is common to all active compliance control schemes and has been noted already by many authors.

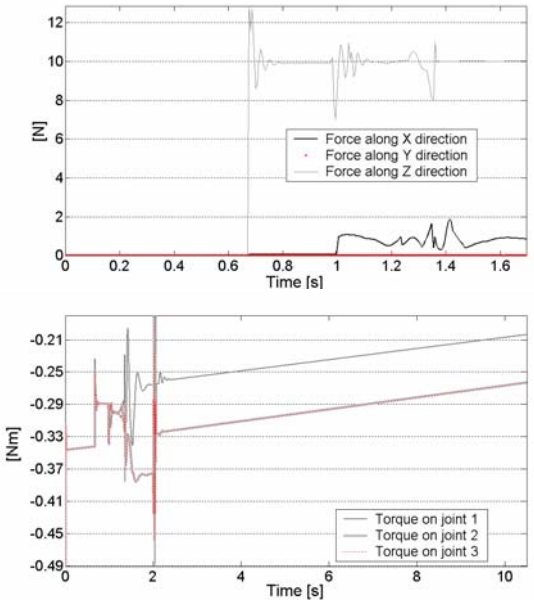

Fig. 15. Contact forces (a) and actuation torques (b) for *1°* misalignment

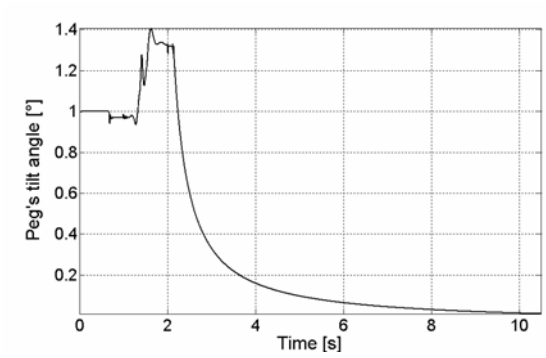

Fig. 16. Trend of peg's slope

VI. Conclusions

The design of the novel *3-RCC* parallel machine, whose kinematics and dynamics had been previously studied, has been assessed with respect to its characterising dynamic performances when operating in constrained conditions: an implicit type of hybrid position/force controller has been developed for the purpose. Many simulations have been performed to assess the behaviour of the robot with the proposed controller when performing tasks characterised by interaction with the environment and finally it has been proven that the special case of the peg-in-hole assembly can be successfully handled; of course, a proper planning of the operation must grant that both jamming and wedging conditions do not establish during the manoeuvre and that the assigned cycle time does not result in too high velocities. It has been also found that if the end-effector orientation is not controlled, misalignments greater than *3°* lead to the practical impossibility to complete the manoeuvre.

VII. Acknowledgement

The research has been supported by funds of the Italian Ministry of Research and Education (MIUR) within the PRIDE Project.

VIII. References

[1] T. Yoshikawa, "Dynamics shaping in robot force control and artificial reality", in *Proc. Intl. Conf. on Advanced Robotics*, Tokyo, 3-8, 1993.

[2] M. Callegari and M. Tarantini, "Kinematic Analysis of a Novel Translational Platform", *ASME Journal of Mechanical Design,* Vol. 125, No. 2, June 2003.

[3] D.E. Whitney. "Quasi-Static Assembly of the Compliantly Supported Rigid Parts", *ASME Journal of Dynamic Systems, Measurement and Control*, Vol. 104, No. 1, 65-77, 1982.

[4] M. Callegari and P. Marzetti, "Kinematics of a family of parallel translating mechanisms", *Proc. 12th Int. Workshop on Robotics in Alpe-Adria-Danube Region*, Cassino, May 7-10, 2003.

[5] M. Callegari and M. Bastianelli, "Dynamics Modelling and Control of the 3-RCC Translational Platform", *IEEE/ASME Transactions on Mechatronics*, considered for publication

[6] J.L. Nevins and D.E. Whitney, *Concurrent Design of Products and Processes*, McGraw-Hill, New York, 1989.

[7] M. Shahinpoor and H. Zohoor, "Analysis of Dynamic Insertion Type Assembly for Manufacturing Automation", *Proc. IEEE Int. Conf. on Robotics and Automation,* Sacramento, U.S.A, April 9-11, 1991, Vol. 3. 2458-2464.

[8] J.P. Merlet, "Force-feedback control of parallel manipulators", *Proc. IEEE Int. Conf. on Robotics and Automation*, Philadelphia, U.S.A., April 24-29, 1988, Vol. 3; 1484-1489.

[9] S.M. Satya, P.M. Ferriera and M.W. Spong, "Hybrid Control of a Planar 3-Dof Parallel Manipulator for Machining Operations", *Transaction of the NAMRI/SME*, 1995, Vol. 23; 273-280.

[10] B. Siciliano, L. Villani, *Robot Force Control*, Kluwer, 2000.